Original Paper

Alterations of auditory sensory gating in mice with noise-induced tinnitus treated with nicotine and cannabis extract

Journal of Psychopharmacology
2023, Vol. 37(11) 1116–1131

DOI: 10.1177/02698811231200879
journals.sagepub.com/home/jop

Barbara Ciralli[1], Thawann Malfatti[1,3], Thiago Z Lima[1,2], Sérgio Ruschi B Silva[1], Christopher R Cederroth[3,4] and Katarina E Leao[1]

Abstract

Tinnitus is a phantom sound perception affecting both auditory and limbic structures. The mechanisms of tinnitus remain unclear and it is debatable whether tinnitus alters attention to sound and the ability to inhibit repetitive sounds, a phenomenon also known as auditory gating. Here we investigate if noise exposure interferes with auditory gating and whether natural extracts of cannabis or nicotine could improve auditory pre-attentional processing in noise-exposed mice. We used 22 male C57BL/6J mice divided into noise-exposed (exposed to a 9–11 kHz narrow band noise for 1 h) and sham (no sound during noise exposure) groups. Hearing thresholds were measured using auditory brainstem responses, and tinnitus-like behavior was assessed using Gap prepulse inhibition of acoustic startle. After noise exposure, mice were implanted with multi-electrodes in the dorsal hippocampus to assess auditory event-related potentials in response to paired clicks. The results showed that mice with tinnitus-like behavior displayed auditory gating of repetitive clicks, but with larger amplitudes and longer latencies of the N40 component of the aERP waveform. The combination of cannabis extract and nicotine improved the auditory gating ratio in noise-exposed mice without permanent hearing threshold shifts. Lastly, the longer latency of the N40 component appears due to an increased sensitivity to cannabis extract in noise-exposed mice compared to sham mice. The study suggests that the altered central plasticity in tinnitus is more sensitive to the combined actions on the cholinergic and the endocannabinoid systems. Overall, the findings contribute to a better understanding of pharmacological modulation of auditory sensory gating.

Keywords

Tinnitus, hippocampus, auditory event-related potentials, ABR, GPIAS

Introduction

Subjective tinnitus is a phantom sound sensation without an external source that is related to comorbidities such as anxiety and depression (Langguth et al., 2011) and decreased quality of life (Hiller and Goebel, 2006). Tinnitus affects around 15% of the world population (Biswas et al., 2022) and so far cognitive behavioral therapy is the only evidence-based recommended treatment (Cima et al., 2019). A relationship between tinnitus and decreased understanding of speech-in-noise has been reported (Tai and Husain, 2019) but it remains unclear whether chronic tinnitus directly interferes with speech-in-noise processing (Zeng et al., 2020), or whether this is a result of attentional problems that have been difficult to assess in tinnitus subjects (Tai and Husain, 2019). The limbic system is implicated in the manifestation and development of chronic tinnitus (Chen et al., 2015), and positron emission tomography and functional magnetic resonance imaging (fMRI) studies have shown greater activation of the auditory cortex, as well as non-auditory areas (frontal areas, limbic system, and cerebellum) in tinnitus patients compared to controls (Lanting et al., 2009). Animal models of tinnitus point to neuronal alterations in the dorsal cochlear nucleus (Shore et al., 2016), affecting upstream auditory nuclei, with previous evidence of altered activity of the auditory cortex (Asokan et al., 2018). The auditory cortex has been shown to have significantly reduced functional connectivity with limbic structures (such as the hippocampus and amygdala) when comparing regional fMRI low-frequency activity fluctuations in a mouse model of noise-induced tinnitus (Qu et al., 2019). Still, the involvement of limbic structures, such as the hippocampus, in noise-induced tinnitus remains poorly investigated.

Auditory information reaches the hippocampus through two distinct pathways: the lemniscal and non-lemniscal pathways,

[1]Brain Institute, Federal University of Rio Grande do Norte, Natal, RN, Brazil
[2]Department of Applied Mathematics and Statistics, Exact and Earth Sciences Center, Federal University of Rio Grande do Norte, Natal, RN, Brazil
[3]Experimental Audiology, Department of Physiology and Pharmacology, Karolinska Institutet, Sweden
[4]Translational Hearing Research, Tübingen Hearing Research Center, Department of Otolaryngology, Head and Neck Surgery, University of Tübingen, Tübingen, Germany

Corresponding author:
Katarina E. Leao, Brain Institute, Federal University of Rio Grande do Norte, Avenue Senador Salgado Filho, 3.000, Campus Universitário Lagoa Nova, Postal box 1524, Natal-RN, CEP 59078-970, Brazil.
Email: katarina.leao@neuro.ufrn.br

which converge in the entorhinal cortex before reaching the hippocampus (Nadhimi and Llano, 2021). Processing of auditory input in the hippocampus can be measured by auditory event-related potentials (aERP) for sensory gating, which is defined as a reduction in aERP to a repeated identical stimulus. Mouse aERP recordings are commonly performed on the CA1 and CA3 hippocampal regions (Ma et al., 2009; Rudnick et al., 2010; Smucny et al., 2015). Notably, the CA1 region maintains direct connections with the primary auditory cortex and auditory association areas (Cenquizca and Swanson, 2007). This unique connectivity establishes the hippocampus as an important interface between the auditory and limbic systems, potentially impacted in neurological conditions such as tinnitus.

Auditory sensory gating can be assessed with paired-click stimuli (0.5 s apart) where the aERP magnitude in response to the second click generates a smaller amplitude compared to the first. In humans, aERPs are measured using electroencephalogram, while in mice aERPs are often recorded using intra-hippocampal chronically implanted electrodes (Amann et al., 2008; Rudnick et al., 2010). An incomplete suppression of the second click represents abnormal sensory processing, and poor "gating" of paired auditory stimuli (Lijffijt et al., 2009). A decrease in sensory gating measured by cortical aERPs in response to paired tones has been shown to be correlated with tinnitus severity in young adults (Campbell et al., 2018), whereas an increased latency in aERP was found in tinnitus patients (dos Santos Filha and Matas, 2010). Still, the neuronal correlates of aERPs are poorly understood and animal models of noise-induced tinnitus measuring auditory gating are largely lacking even though the aERP waveform of rodents, described as positive (P) or negative (N) peaks, with approximate latency in milliseconds, P20, N40, and P80 (Amann et al., 2008) or P1, N1, and P2, are analogous to the human waveforms (P50, N100, and P200).

Pharmacologically, it has been shown that certain nicotinic acetylcholine receptors take part in augmenting aERPs (Amann et al., 2008; Rudnick et al., 2010). Furthermore, it was shown that smoking cigarettes containing different doses of cannabis led to a reduction in the amplitude of event-related potentials. Additionally, subjects experienced an acutely diminished attention and stimulus processing after smoking cannabis (Bäcker et al., 2010). On the contrary, a combined activation of the cholinergic and the endocannabinoid system has shown to improve auditory deviant detection and mismatch negativity aERPs in human subjects, but not when each drug was delivered alone (de la Salle et al., 2019). This indicates interactions between the two systems; however, the impact of nicotine and/or cannabis, on aERPs in animal models of tinnitus, has to our knowledge not yet been studied. Here, we first hypothesized that noise-induced tinnitus interferes with auditory gating, and next that nicotine or natural extracts of cannabis could improve auditory pre-attentional processing in noise-induced tinnitus. To test this, we used a mouse model of noise-induced tinnitus without hearing impairment and measured aERPs in the dorsal hippocampus in response to paired clicks.

Methods

Animals

All protocols were approved by and followed the guidelines of the ethical committee of the Federal University of Rio Grande do Norte, Brazil (Comitê de Ética no Uso de Animais — CEUA; protocol no.094.018/2018). C57BL/6J male mice (1 month old at the beginning of the experimental timeline) originated from an in-house–breeding colony. Here we used a total of 29 mice, where 7 were excluded in the Gap-prepulse inhibition of acoustic startle (GPIAS) test initial screening due to poor GPIAS (see exclusion criteria at the GPIAS section), leading to a total of 22 mice reported in all experimental procedures. Before the beginning of experiments, the animals were randomly assigned using python scripts (see Section "Histology") to the Sham ($n = 11$) or Noise-exposed ($n = 11$) group. From those, three animals were excluded from aERP recordings due to low signal-to-noise ratio and two animals died after surgery (remaining 10 Sham and 7 Noise-exposed). Animals were housed on a 12/12 h day/night cycle (onset/offset at 6 h/18 h) at 23°C to maintain normal circadian rhythm and had free access to water and food pellets based on corn, wheat, and soy (Nuvilab, Quimtia, Brazil: #100110007, Batch: 0030112110). All experiments were performed during the day cycle, ranging from 7 h to 15 h. Animals (2–4 per cage) were housed in individually ventilated cages, and paper and a polypropylene tube were added as enrichment. Once implanted, animals were single-housed until the end of the experiment. Mice were tunnel-handled for the experiments as it has been shown to impact stress during experimental procedures, while tail-handling was used for routine husbandry procedures.

Sound calibration

The sound equipment used for Auditory brainstem responses (ABRs), noise exposure, GPIAS, and aERPs was calibrated in their respective arenas, all inside a sound-shielded room with background noise of 35-decibel sound pressure level (dBSPL). We used an ultrasonic microphone (4939-A-011, Brüel and Kjær) to record each of the stimuli used at 300 voltage steps logarithmically spaced in the 0–1 V range, allowing to play all needed stimuli at the voltage necessary to achieve the needed intensity in dBSPL.

Auditory brainstem responses

The ABRs of mice were tested both before and after the noise exposure protocol. Mice were anesthetized with an intraperitoneal injection (10 µl/gr) of a mixture of ketamine/xylazine (90/6 mg/kg) plus atropine (0.1 mg/kg) and placed in a stereotaxic apparatus on top of a thermal pad with a heater controller (Supertech Biological Temperature Controller, TMP-5b) set to 37°C and ear bars holding in front of and slightly above the ears, on the temporal bone, to not block the ear canals. The head of the animal was positioned 11 cm in front of a speaker (Super tweeter ST400 trio, Selenium Pro). To record the ABR signal, two chlorinated electrodes were used, one recording electrode and one reference (impedance 1 kΩ) placed subdermally into small incisions in the skin covering the bregma region (reference) and lambda region (recording). The sound stimulus consisted of narrow-band uniform white noise pulses with lengths of 3 ms each, presented at 10 Hz for 529 repetitions at each frequency and intensity tested. The frequency bands tested were: 8–10 kHz, 9–11 kHz, 10–12 kHz, 12–14 kHz, and 14–16 kHz. Pulses were presented at 80 dBSPL in decreasing steps of 5 dBSPL to the final intensity 45 dBSPL as previously described (Malfatti et al., 2022). The experimenter was blinded to the animal group during the ABR recordings.

Gap prepulse inhibition of acoustic startle

The GPIAS test (Turner et al., 2006) is known to reliably measure tinnitus-like behavior in rodents such as rats, mice, and guinea pigs (Longenecker and Galazyuk, 2012, 2016; Longenecker et al., 2018; Park et al., 2020), and was used here to infer tinnitus in noise-exposed mice. GPIAS evaluates the degree of inhibition of the auditory startle reflex by a short preceding silent gap embedded in a carrier background noise. Before the first recording session, the animals were habituated to the experimenter and experimental setup for three consecutive days. Then, mice were acclimatized during the next three consecutive days by running the entire GPIAS session with all frequencies and trials but without the startle pulse. Animals were allowed 5 min inside the recording chamber before each recording session. Mice were then screened 3 days before the noise exposure for their ability to detect the gap. Animals were then tested again 3 days after noise exposure or sham procedures (no noise), as previously described (Malfatti et al., 2022). Animals were placed in custom-made acrylic cylinders perforated at regular intervals. The cylinders were placed in a sound-shielded custom-made cabinet ($44 \times 33 \times 24$ cm) with low-intensity LED lights in a sound-shielded room with ≈35 dBSPL (*Z*-weighted) of background noise. A single loudspeaker (Super tweeter ST400 trio, Selenium Pro, freq. response 4–18 kHz) was placed horizontally 4.5 cm in front of the cylinder, and startle responses were recorded using a digital accelerometer (MMA8452Q, NXP Semiconductors, Nijmegen, Netherlands) mounted to the base plate of the cylinder and connected to an Arduino Uno microcontroller, and a data acquisition cart (Open-Ephys board) analog input. Sound stimuli consisted of 60 dBSPL narrow-band filtered white noise (carrier noise); 40 ms of a silent gap (GapStartle trials); 100 ms of inter-stimulus interval carrier noise; and 50 ms of the same noise at 105 dBSPL (startle pulse), with 0.2 ms of rise and fall time. The duration of the carrier noise between each trial (inter-trial interval) was pseudo-randomized between 12 and 22 s. Test frequencies between 8–10, 9–11, 10–12, 12–14, 14–16, and 8–18 kHz were generated using a Butterworth bandpass filter of 3rd order. The full session consisted of a total of 18 trials per frequency band tested (nine Startle and nine GapStartle trials per frequency, pseudo-randomly played). It was previously shown that mice can suppress at least 30% of the startle response when the loud pulse is preceded by a silent gap in background noise (Li et al., 2013); therefore, we retested frequencies to which an animal did not suppress the startle by at least 30% in a second session the next day. Animals that still failed to suppress the startle following the silent gap in at least two frequencies in the initial GPIAS screening were excluded from further experiments. The experimenter was blinded to the animal group during the GPIAS recordings. Since we only assessed mice three days after noise exposure, while others suggest that chronic tinnitus arises after 7 weeks in C57Bl6 mice (Turner et al., 2012), we infer our GPIAS relates to acute tinnitus.

Noise exposure

Mice were anesthetized with an intraperitoneal administration of ketamine/xylazine (90/6 mg/kg), placed inside an acrylic cylinder (4×8 cm) facing a speaker (4 cm distance) inside a sound-shielded cabinet ($44 \times 33 \times 24$ cm) and exposed to a narrow-band white noise filtered (Butterworth, −47.69 dBSPL/Octave) from 9 to 11 kHz, at an intensity of 90 dBSPL for 1 h. This protocol was previously shown to trigger a tinnitus-phenotype in C57BL/6 mice that could be decreased by chemogenetically modulating the firing rate of CaMKIIα + dorsal cochlear nucleus (DCN) units (Malfatti et al., 2022). Next, mice remained in the cylinder inside the sound-shielded chamber for 2 h, due to the fact that sound-enrichment post loud noise exposure may prevent tinnitus induction (Sturm et al., 2017). Sham animals were treated equally, but without any sound stimulation. We used 11 noise-exposed and 11 sham animals. The animals were then returned to their home cages.

Electrode array assembly

Tungsten-insulated wires of 35 µm diameter (impedance 100–400 kΩ, Grover Beach, California Wires Company) were used to manufacture 2×8 arrays of 16 tungsten wire electrodes. The wires were assembled to a 16-channel custom-made printed circuit board and fitted with an Omnetics connector (NPD-18-VV-GS). Electrode wires were spaced by 200 µm with increasing length distributed diagonally in order to record from different hippocampal layers, such that, after implantation, the shortest wire was at dorsoventral (DV) depth of −1.50 mm and the longest at DV −1.96 mm. The electrodes were dipped in fluorescent dye (1,1′-dioctadecyl-3,3,3′,3′-tetramethylindocarbocyanine perchlorate; DiI, Invitrogen) for 10 min (for post hoc electrode position) before implanted into the right hemisphere hippocampus.

Electrode array implantation

Twenty-two animals were used for the electrode implantation surgery. In detail, mice were anesthetized using a mixture of ketamine/xylazine (90/6 mg/kg) and placed in a stereotaxic frame on top of a heat pad (37°C). Dexpanthenol was applied to cover the eyes to prevent ocular dryness. When necessary, a bolus of ketamine (45 mg/kg) was applied during surgery to maintain adequate anesthesia. Iodopovidone 10% was applied on the scalp to prevent infection, and 3% lidocaine hydrochloride was injected subdermally before an incision was made. In order to expose the cranial sutures, 3% hydrogen peroxide was applied over the skull. Four small craniotomies were done in a square at coordinates mediolateral (ML) 1 mm and anteroposterior (AP) −2.4 mm; ML: 1 mm and AP: −2.6 mm; ML: 2.45 mm and AP: −2.4 mm; ML: 2.45 mm and AP: −2.6 mm, to make a cranial window where the electrodes were slowly inserted at DV coordinate of −1.96 mm (for the longest shank). Four additional holes were drilled for the placement of anchoring screws, where the screw placed over the cerebellum served as reference. The electrode implant was fixed to the skull with polymethyl methacrylate moldable acrylic polymer around the anchor screws. After surgery, the animals were monitored until awake and then housed individually and allowed to recover for 1 week before recordings. For analgesia, ibuprofen 0.04 mg/ml was administered in the water bottle 2 days before and 3 days after the surgery. Subcutaneous Meloxicam 5 mg/kg was administered for three consecutive days after the surgery. Two animals died shortly after the surgery, remaining 10 animals in the sham group and 7 in the noise-exposed group.

Paired-click stimuli for auditory event-related potentials

Mice were habituated during 2 days in the experimental setup and in the day of recording, anesthesia was briefly induced with isoflurane (5% for <1 min) to gently connect the implanted electrode array to a head-stage (Intan RHD 2132) connected to an acquisition board (XEM6010-LX150 v2.2, OpenEphys, Lisbon) by a thin flexible wire. aERPs were recorded in freely moving animals placed in a low-light environment exposed to paired click stimulus, played by a speaker (Selenium Trio ST400) located 40 cm above the test area. All recordings were performed in standard polycarbonate cage bottom, which was placed inside a sound-shielded box (40 × 45 × 40 cm). The paired clicks consisted of white noise filtered at 5–15 kHz presented at 85 dBSPL, 10 ms of duration with 0.2 ms rise/fall ramp, and 0.5 s interstimulus interval. Stimulus pairs were separated by 2–8 s (pseudorandomly), and a total of 50 paired stimuli were presented. The session duration varied from 148 s to 442 s.

To investigate aERPs, average data from different animals, and also, compare responses from different experimental days and different pharmacological treatments, the appropriate hippocampal location for picking up aERP was identified. As local field potentials are related to cell density, and thereby the resistivity of the tissue, it is useful to record from the hippocampus with its distinct layered structure that shows phase-reversals of local field potentials (Scheffer-Teixeira et al., 2011). Responses to paired clicks were recorded 1 week after surgery. The grand average of aERP (average of 50 clicks) for each channel was plotted and the changed signal polarity across hippocampal layers was identified, as the electrode array channels were distributed at different depths. To facilitate comparison of aERP between implanted animals we selected the first channel above phase reversal that showed a clear negative peak followed by a positive peak in the deeper channel. The visualization of the phase reversal channel was routinely added to analysis as channels sometimes shifted in the same animal, likely due to small movements in the electrode array when connecting/disconnecting mice to/from the headstage during different recording sessions. The experimenter was blind to the animal group during the aERP recordings.

Cannabis sativa *extract production and analysis*

Δ^9 tetrahydrocannabinol (THC) is the main psychoactive compound in cannabis and it is known to be partial agonist of cannabinoid receptor types 1 and 2 (CB1 and CB2) (Sampson, 2020), while cannabinol (CBN) activates CB1 and CB2 receptors with more affinity over the latter and canabidiol (CBD) acts as a negative allosteric modulator of CB1 (Sampson, 2020). The *Cannabis sativa* extract was produced from an ethanolic extraction with the flowers previously dried and crushed. After leaving them in contact with the solvent for 5 min in an ultrasonic bath, filtration was performed and the process was repeated twice. Additionally, the solvent was evaporated and recovered, leaving only the cannabis extract in resin form. Decarboxylation of the acidic components, mainly tetrahydrocannabinolic acid into THC, was carried out by heating the material at 90°C until the conversion to the neutral forms had been completed. The cannabis extract was analyzed by high-performance liquid chromatography (HPLC). Analytical standards of THC (Cerilliant T-005), CBN (Cerilliant C-046), and CBD (Cerilliant C-045) were used in the calibration curve dilutions. An Agilent 1260 LC system (Agilent Technologies, Mississauga, ON, Canada) was used for the chromatographic analysis. A Poroshell 120 EC-C18 column (50 mm × 3.0 mm, 2.7 µm, Agilent Technologies) was employed, with a mobile phase at a flow rate of 0.5 ml/min and temperature at 50°C (separation and detection). The compositions were (A) water and (B) methanol. 0.1% formic acid was added to both water and methanol. The total analysis time was 18 min with the following gradient: 0–10 min, 60–85%B; 10–11 min, 85–100%B; 11–12 min, 100%; 12–17 min, 100–60%; 17–18 min, 60% the temperature was maintained at 50°C (separation and detection). The injection volume was 5 µL and the components were quantified based on peak areas at 230 nm. During the experiments, we used a single dose of cannabis extract for each animal (100 mg/kg), containing 47.25 mg/kg of THC; 0.43 mg/kg of CBD and 1.17 mg/kg of CBN as analyzed by HPLC, and kindly donated by the Queiroz lab, Brain Institute, Federal University of Rio Grande do Norte, Brazil.

Pharmacology

To activate the cholinergic system, and specifically brain nicotinic acetylcholine receptors, animals received a single intraperitoneal injection of nicotine (Sigma N3876) at 1.0 mg/kg (Metzger et al., 2007) or saline (randomized order, 2 days in between session 1 and 2) 5 min before aERP recordings. In comparison to nicotine, which has a half-life of approximately 6–7 min in mouse plasma (Petersen et al., 1984), THC, CBD, and CBN have longer half-lives. Specifically, THC has a half-life of approximately 110 min in mouse plasma (Torrens et al., 2020), CBD has a half-life of 3.9 h in mouse plasma (Xu et al., 2019), and CBN has a half-life of 32 h in human plasma (Johansson et al., 1987). Here, we administered a single dose of cannabis extract (100 mg/kg) and recorded responses after 30 min, similar to previously reported (Dissanayake et al., 2008; El-Alfy et al., 2010; Kasten et al., 2019). On the experimental day, the cannabis extract resin was diluted in corn oil to 10 mg/ml solution by mixing the extract and the oil and then sonicating for 5 min before injecting intraperitoneally (at +volume of 10 µl/g body weight) 30 min prior to aERP recording sessions to reach max plasma concentration of THC (Torrens et al., 2020). After the third recording session, an additional dose of nicotine (1 mg/kg) was injected (to study potentially synergistic effects of cannabis extract + nicotine) and the animals were recorded 5 min later to observe how the interaction of the cholinergic and endocannabinoid system affects aERPs. After each aERP recording session, mice were unconnected from the headstage and returned to their home cage.

Histology

To verify expected electrode positioning, animals were deeply anesthetized at the end of the experimental timeline with a mixture of ketamine/xylazine (180/12 mg/kg) and transcardiac perfused with cold phosphate-buffered saline followed by 4% paraformaldehyde (PFA). Brains were dissected and placed in 4% PFA for 48 h. Next, brains were sliced using a free-floating vibratome (Leica VT1000S) at 75 µm thickness, and cell nuclei

were stained with 4′,6-diamidino-2-phenylindole (DAPI, Sigma) to visualize cell layers and borders of the hippocampus. In addition to DiI-staining the electrodes, a current pulse of 500 µA was routinely passed through the deepest electrode for 5 s at the end of the last aERP recordings to cause a small lesion around the electrode tip to confirm electrode depth. Images were visualized using a Zeiss imager A2 fluorescence microscope with a N-Achroplan 5x objective.

Data analysis

Analysis of ABRs was done as previously described (Malfatti et al., 2022) and consisted of averaging the 529 trials, filter the signal using a 3rd-order Butterworth bandpass filter from 600 to 1500 Hz, and slice the data 12 ms after the sound pulse onset. Thresholds were defined by automatically detecting the lowest intensity that can elicit a wave peak one standard deviation above the mean, and preceded by a peak in the previous intensity (Malfatti et al., 2022). The effect of noise exposure and frequency of stimulus on ABR thresholds was evaluated using the Friedman Test, and pairwise comparisons were performed using the Wilcoxon signed-rank test. The effect of group was evaluated using the Kruskal–Wallis test, and pairwise comparisons were performed using the Mann–Whitney U test. The effect of group and frequency of stimulus on ABR threshold differences before and after exposure was evaluated using two-way analysis of variance (ANOVA). When multiple comparisons within the same dataset were performed, p values were Bonferroni-corrected accordingly.

For each frequency tested in GPIAS, Startle, and GapStarle trials responses were separated and the signal was filtered with a Butterworth lowpass filter at 100 Hz. The absolute values of the accelerometer axes, from the accelerometer fitted below the cylinders enclosing the mice during the modified acoustic startle test, were averaged and sliced 400 ms around the startle pulse (200 ms before and 200 ms after). The root-mean-square (RMS) of the sliced signal before the Startle (baseline) was subtracted from the RMS after the startle response (for both Startle only and GapStartle sessions). The GPIAS index for each frequency was then calculated as

$$\left(1-\left(\frac{\text{GapStartle RMS}}{\text{Startle RMS}}\right)\right)*100$$

generating percentage of suppression of startle. For each animal, the most affected frequency was determined as the frequency with the greatest difference in GPIAS index before and after noise exposure. This was done as mice did not show decreased GPIAS at the same narrow-band frequency despite being subjected to the same noise exposure, indicating individual differences in possible tinnitus perception (Longenecker and Galazyuk, 2016). The definition of the most affected frequency followed the same procedure for both sham and noise-exposed animals. The effects of group (sham or noise-exposed), epoch (before or after exposure), and frequency of stimulus were tested using three-way mixed models ANOVA. The effect of the group and epoch on the GPIAS index of the most affected frequency was evaluated using the Kruskal–Wallis and the Friedman test, respectively; and pairwise comparisons were done using the Mann–Whitney U and Wilcoxon signed-rank test, respectively.

aERP in response to paired-clicks were filtered using a low pass filter at 60 Hz, sliced 0.2 s before and 1 s after the first sound click onset, and all 50 trials were averaged. To compare signals between different animals ($n = 10$ sham and $n = 7$ noise-exposed) and different treatments, we always analyzed the channel above hippocampal phase reversal with a negative peak around 40 ms (N40) and a positive peak around 80 ms latency (P80). aERP components were quantified by peak amplitude (baseline-to-peak) after stimulus onset. The N40 was considered as the maximum negative deflection between 20 and 50 ms after the click stimulus, and P80 as the maximum positive deflection after the N40 peak. The baseline was determined by averaging all 50 trials and then averaging the 200 ms of prestimulus activity (before the first click). The latency of a component was defined as the time of occurrence of the peak after stimulus onset. The ratio in percentage of the first and second click amplitude (the suppression of the second click, for example, sensory filtering) was calculated as

$$\left(1-\left(\frac{\text{Second Click Amplitude-Baseline}}{\text{First Click Amplitude-Baseline}}\right)\right)*100$$

and error bars represent standard error of the mean (SEM) for all figures. A gating improvement was considered when the aERP peak amplitude suppression ratio(s) increased compared to sham (when comparing between groups) or to saline (when comparing between treatments). The effect of group, treatment, and click on amplitude and latency of aERP components were evaluated using three-way mixed-models ANOVA; effect of group and treatment in aERP components suppression, delay, and N40-P80 width were evaluated using two-way mixed-models ANOVA; and Student's t-test was used for pairwise comparisons. Whenever the response failed to comply with normality, homoscedasticity, and independence assumptions and parametric fitting was inadequate, the Kruskal–Wallis test was used to evaluate the effect of group, and the Mann–Whitney U test was used for pairwise comparisons; and the Friedman test was used to evaluate the effect of treatment and click, and Wilcoxon signed-rank test was used for pairwise comparisons. Statistical power for the tests ranged from 78.5% to 92.2%, and post hoc multiple comparisons were adjusted by Bonferroni correction. Differences in occurrence of double-peak responses were evaluated using McNemar's test.

Recordings were done using the Open-Ephys GUI (Siegle et al., 2015). Stimulation and data analysis were performed using SciScripts (Malfatti, 2023), Scipy (Virtanen et al., 2020), and Numpy (Harris et al., 2020). All plots were produced using Matplotlib (Hunter 2007), and schematics were done using Inkscape (Inkscape Project, 2022). All scripts used for recordings and analysis are available online (Ciralli et al., 2022).

Results

In order to investigate whether noise-exposure can affect auditory gating, we established an experimental timeline for experiments evaluating auditory perception using three different tests in mice exposed to a mild noise (90 dBSPL, 9–11 kHz, 1 h): ABRs, GPIAS, and aERPs. Hearing thresholds of mice were assessed using ABRs 2 days before (baseline) and 2 days after sham or noise exposure (Figure 1(a)). ABRs showed field potentials with distinct peaks indicating neuronal activity at the auditory nerve, cochlear nuclei, superior olivary complex, and inferior colliculus (Henry, 1979) in response to sound clicks presented at different frequencies (Figure 1(b) and (c)). Similar to sham, noise exposure did not cause any change in ABR hearing

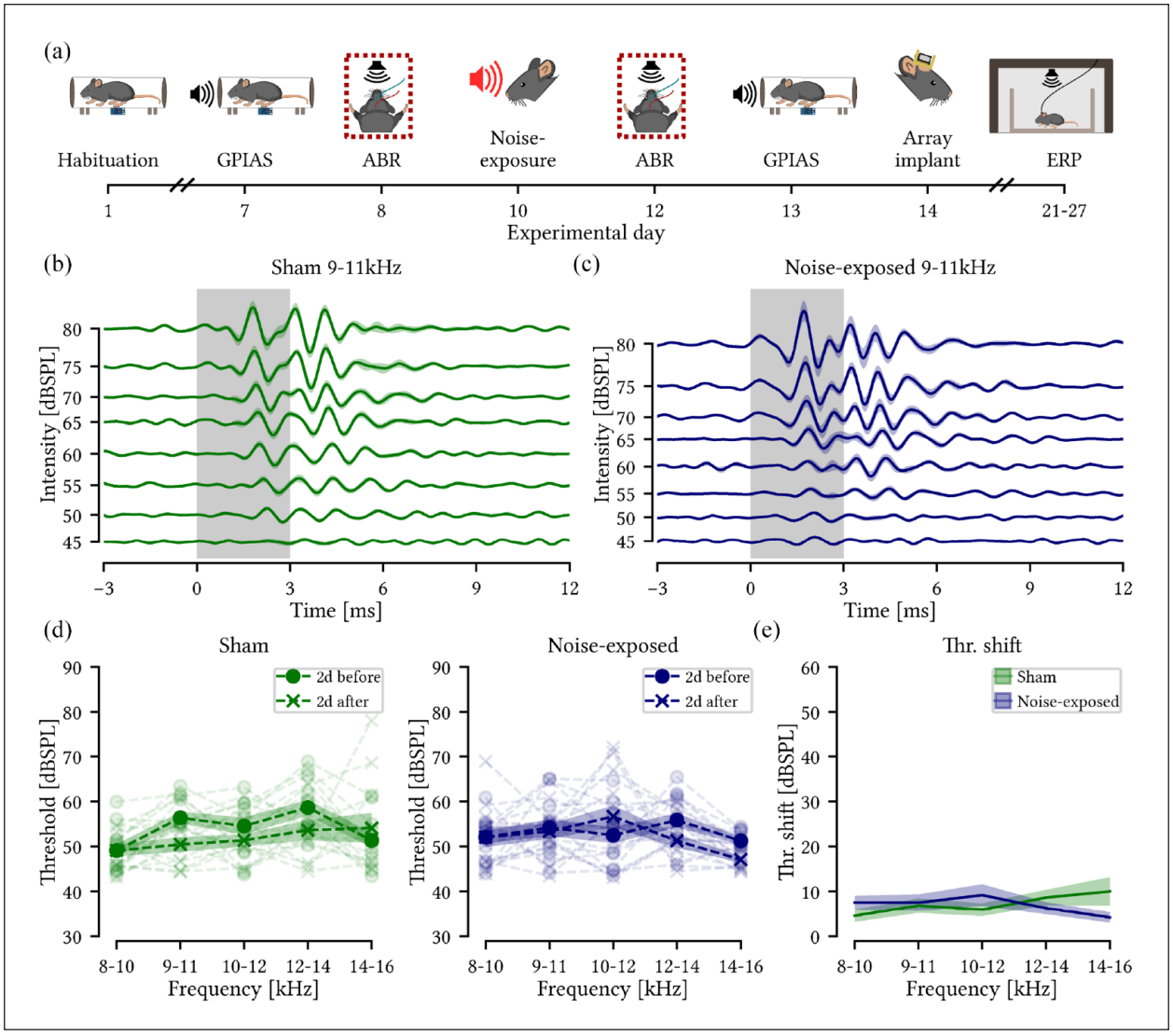

Figure 1. Noise exposure did not cause hearing threshold shift. (a) Full experimental timeline highlighting time of ABR recordings (dotted rectangle). (b and c) Mean ABR to 9–11 kHz after noise-exposure for intensities 45–80 dBSPL for all 529 trials of all sham mice (b) and noise-exposed animals (c). Shaded traces show SEM, gray square indicates the sound pulse duration. (d) Mean+SEM (line and shade) displaying auditory thresholds quantified for sham ($n=11$, left) and noise-exposed ($n=11$, right) animals 2 days before and 2 days after noise exposure, showing no significant difference at any frequency tested (Wilcoxon signed-rank test, $p>0.05$ for all frequencies in both groups). (e) Mean+SEM (line and shade) threshold shift for sham and noise-exposed mice showing no significant difference between groups at any frequency (Student's *t*-test, $p>0.05$ for all frequencies).

thresholds at all frequencies tested when compared to baseline (Group, Kruskal–Wallis eff. size=4.1e−05, $p=0.923$; Epoch, Friedman eff. size=0.058, $p=0.08$; Frequency, Friedman eff. size=0.007, $p=0.164$; Figure 1(d)). When plotting threshold shifts, we confirmed that noise-exposed animals were impacted to a similar degree than sham mice (ANOVA; Group, $F(1,21)=0.047$, $p=0.83$; Frequency, $F(4,84)=0.2$, $p=0.938$; Group:Frequency, $F(4,84)=2.021$, $p=0.09$; Figure 1(e)). Unlike other models of tinnitus (Zhang et al., 2020), we did not detect any effect of noise exposure in ABR Wave 1 amplitude (Epoch, Friedman test, eff. size=0.037, $p=0.118$; Group, Kruskal–Wallis test, eff. size=0.0002, $p=0.821$) or Wave 5 latency (Epoch, Friedman eff. size=0.002, $p=0.55$; Group, Kruskal–Wallis eff.size=0.014, $p=0.073$, Supplemental Figure S1). These findings confirm that the noise exposure did not cause any detectable change in hearing thresholds, and suggest a negligible impact on cochlear synaptopathy.

Three days before and 3 days after noise exposure, mice were tested for GPIAS (Figure 2(a)–(c)). No effect of group (sham or noise-exposed), epoch (before or after noise exposure procedure), or frequency of stimulus was found in GPIAS when evaluating all frequencies from every animal (the closest to significance being the stimulus frequency factor; $F(5,65)=1.419$, $p=0.229$; Figure 2(d) and (e)) and no pairwise differences between any group, epoch, or frequency, possibly due to each individual mouse may experience a different tinnitus pitch. We, therefore, evaluated the background frequency that interferes most with gap prepulse startle suppression for each individual mouse, which

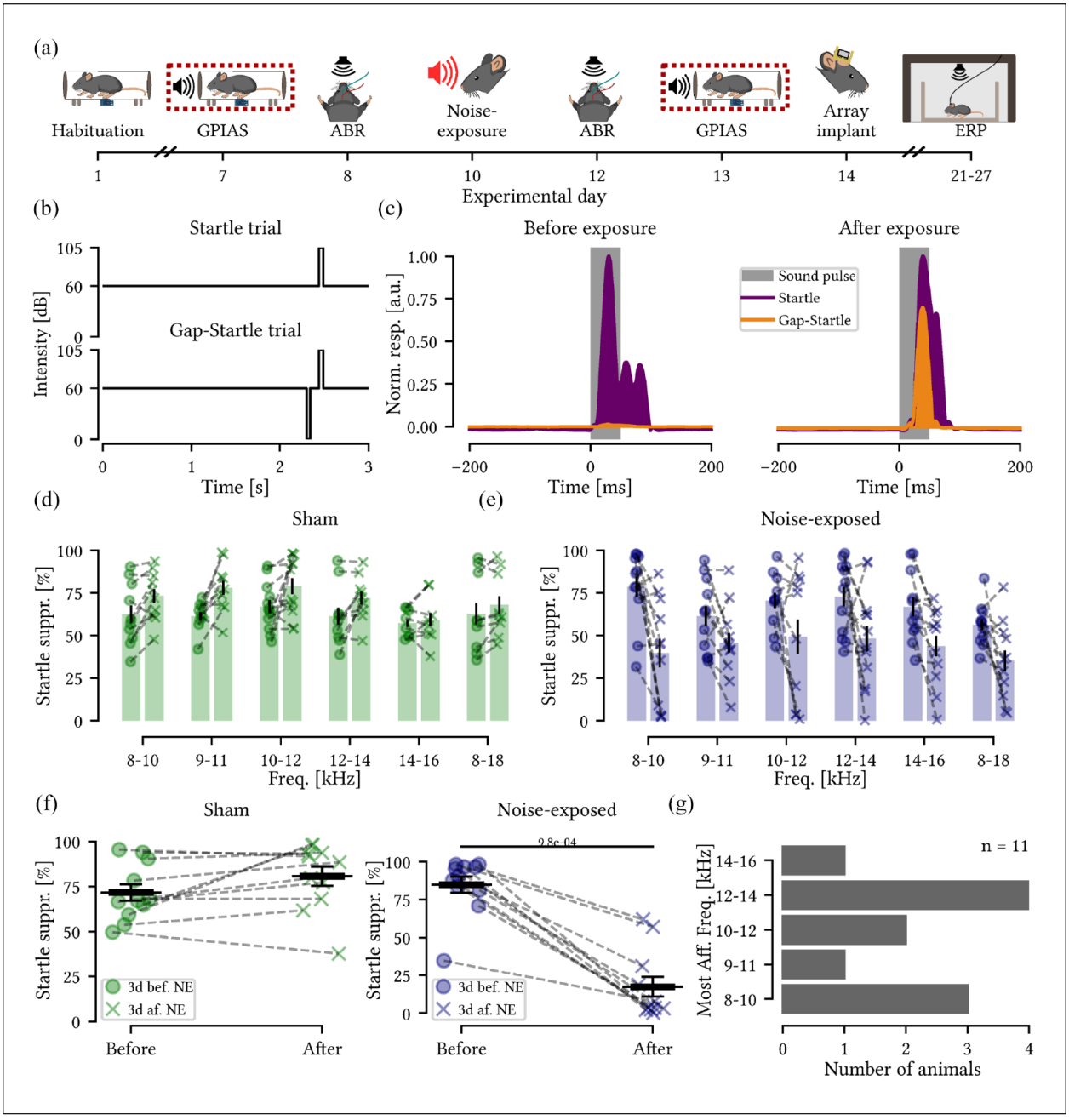

Figure 2. Noise-exposed animals showed decreased startle suppression. (a) Timeline of experiments highlighting time point of the GPIAS tests. (b) Schematic GPIAS protocol. (c) Representative examples of startle suppression by the gap (left) and negative startle suppression (right) from the same animal 3 days before and 3 days after noise exposure, respectively. Filled traces represent an average of nine trials of stimulus without gap (purple) and with gap (orange). Gray rectangle represents the 50 ms startle stimulus. (d and e) GPIAS index for all frequencies tested 3 days before (o) and 3 days after (x) noise exposure for sham (d) and noise-exposed (e) mice. (f) The frequency with largest difference in startle suppression before and after noise-exposure was used for quantification of group GPIAS performance. Sham animals show no difference in GPIAS performance before and after noise exposure (left, $n=11$), while noise-exposed mice (right) show a significant decrease in startle suppression by the silent gap (Wilcoxon signed-rank test, $n=11$, $p=9.8e{-}04$). (g) The frequency with largest difference in startle suppression before and after noise-exposure varied between individual noise-exposed mice.

would correspond to the most likely tinnitus pitch of these animals (Figure 2(f) and (g)). Sham exposure had no effect on GPIAS (Friedman test; eff.size=0.075; $p=0.365$; Figure 2(f), left), while in noise-exposed mice the noise exposure had a significant effect in GPIAS index (Friedman test; eff. size=1.0; $p=1.8e{-}03$), showing a decrease in startle suppression when comparing before and after noise exposure (Wilcoxon signed-rank test, $p=9.8e{-}04$; Figure 2(f), right). Accordingly, the group

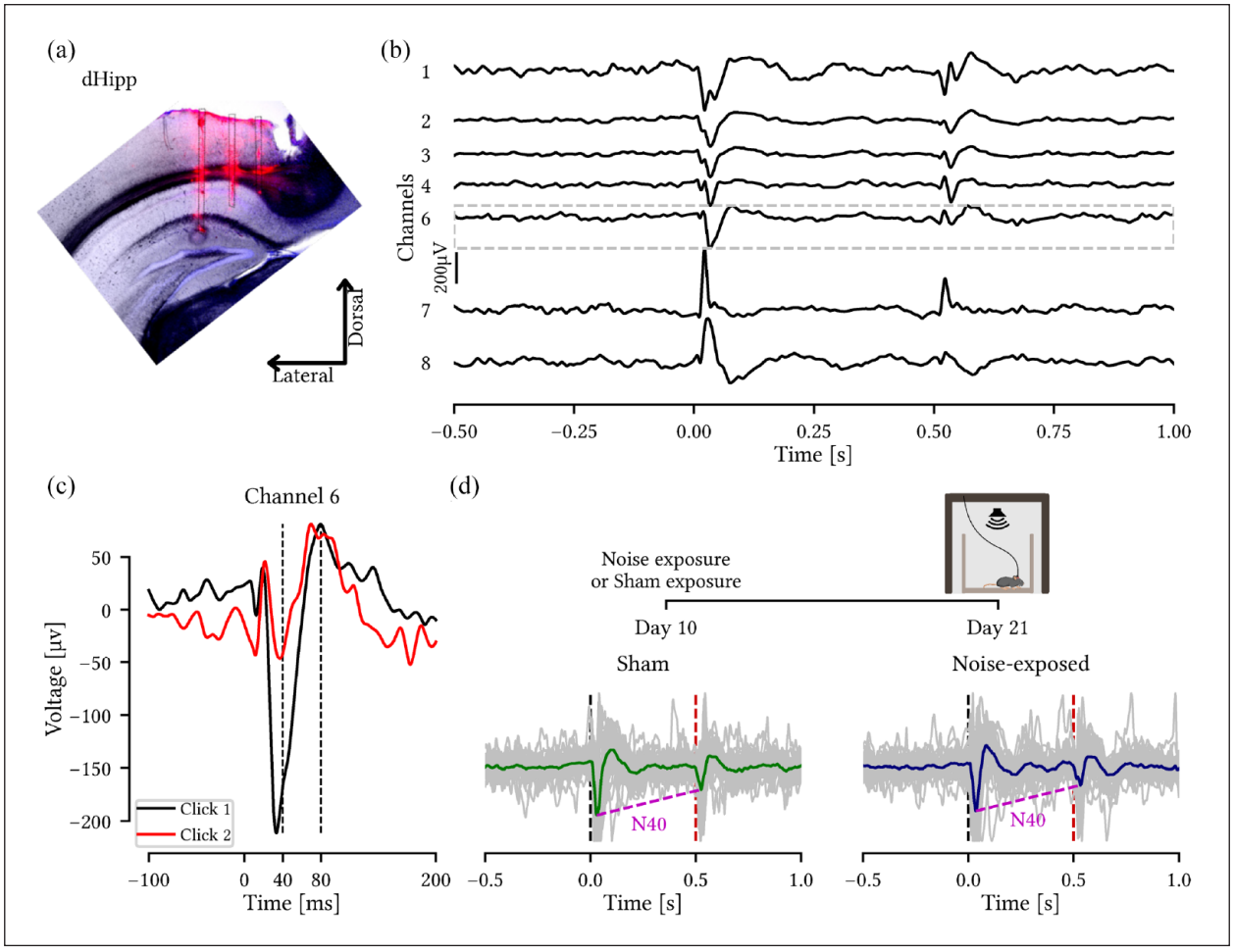

Figure 3. aERP in sham and noise-exposed mice. (a) Coronal slice showing the dorsal hippocampus with electrode tracts stained with DiI in the CA1 region. (b) Average aERPs in response to paired clicks from eight channels at different depths from a recording session from a single animal. The channel above phase reversal (gray dotted box) was consistently used for aERP quantification. (c) The reversal channel from "B" at a greater magnification with click 1 (black) and 2 (red) responses superimposed. Dashed lines indicating positive and negative peaks at different characteristic latencies (N40 and P80 components). (d) Top, simplified experimental timeline. Bottom, average traces of click responses in saline condition for sham (green, $n=10$) and noise-exposed animals (blue, $n=7$). Superimposed gray traces are the average response of 50 trials from each individual animal, dashed lines indicate the sound stimuli onset and amplitude difference of N40 peaks.

(sham versus noise-exposed) had a significant effect on GPIAS measured after noise exposure (Kruskal–Wallis; eff. size = 0.663, $p=3.2e{-}04$), with noise-exposed mice showing lower GPIAS suppression than sham mice (Mann–Whitney U; eff. size = 0.805; $p=4.0e{-}05$); but not before noise exposure (Kruskal–Wallis; eff. size = 0.117, $p=0.066$). GPIAS showed individual variability in the most affected frequency (Figure 2(g)), consistent with previous reports (Longenecker and Galazyuk, 2016) and confirms that tinnitus interferes with the ability to suppress the startle response in noise-exposed animals.

After the ABR and GPIAS tests, electrodes were implanted in the dorsal hippocampus for the assessment of sensory gating (Figure 3(a)). As expected, aERP recordings showed that the second click consistently generated a smaller aERP (Figure 3(b)), and the magnitude of peaks around 40 ms and 80 ms were quantified from baseline as the N40 and P80 peak, respectively, for both the first and second click in the phase-reversal channel (see Methods, Figure 3(b) and (c)). Next, to investigate the impact of noise-induced tinnitus on auditory gating (11 days after noise-exposure), freely exploring mice were individually subjected to randomized paired-click stimuli, where both sham and noise-exposed mice presented characteristic aERP (Figure 3(d)). Two types of measurements were evaluated: the responses to sound clicks measured in the hippocampus (amplitude in µV and latency in ms), which is a measurement of sound processing in the limbic system; and the ratio between the second and the first click responses (both amplitude and latency unitless), which measures the sensory gating.

As attention is modulated by the cholinergic system (Ballinger et al., 2016) and also the endocannabinoid system (Verrico et al., 2003), we tested the impact of two agonists to both systems (nicotine and cannabis extract, individually or in combination) in

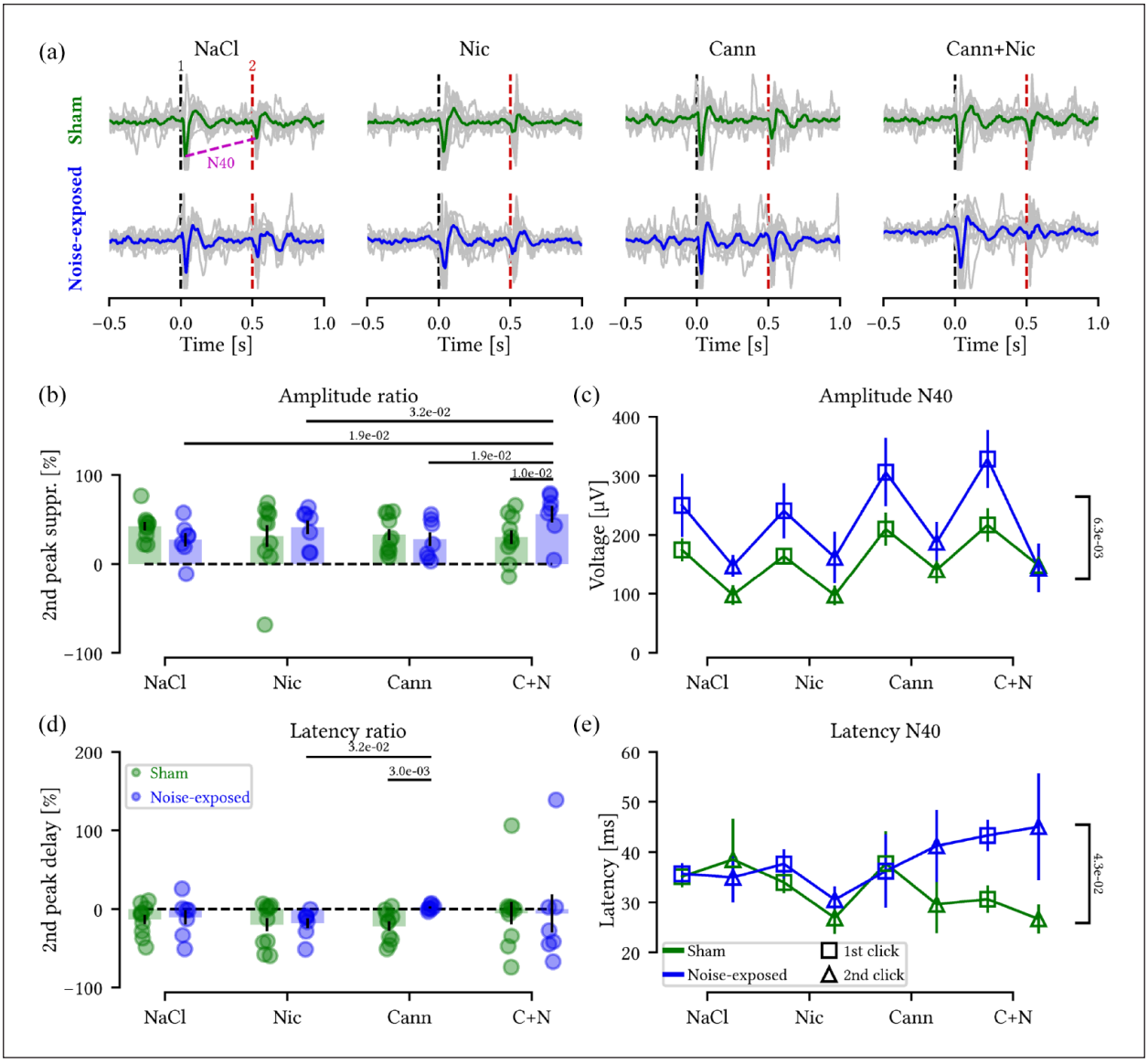

Figure 4. Noise-exposed mice have improved auditory gating under cannabis + nicotine treatment and showed overall larger and slower ERP responses. (a) Auditory ERP recorded in awake mice in response to saline, nicotine, cannabis, and cannabis + nicotine show characteristic suppression of the second click in both sham (top) and noise-exposed (bottom) animals. Gray trace shows the average aERP per animal while the green and blue traces show the group average for each treatment. (b) Percentage of suppression of the second click of the N40 component (Supplemental Figure S2) for sham (green) and noise-exposed (blue) mice, showing largest suppression of the second peak in noise-exposed mice following cannabis + nicotine administration (Student's *t*-test). (c) N40 amplitude is consistently increased for noise-exposed ($n=7$) compared to sham animals ($n=10$). (d) Percentage of the second N40 peak delay for both groups at each treatment showed cannabis extract to increase delay in noise-exposed mice compared to sham (Mann–Whitney U test), as well as compared to nicotine treatment of noise-exposed mice (Wilcoxon signed-rank test). (e) N40 latency is consistently increased for noise-exposed ($n=7$) compared to sham animals ($n=10$).

modulation of aERPs in our model of noise-induced tinnitus (Figure 4(a)). Animals were given a single injection of nicotine (1 mg/kg) or saline before aERP recordings on the first two sessions. During the third session, the remaining two aERP recordings were conducted, with the initial recording taking place 30 min after the administration of cannabis extract (100 mg/kg). Subsequently, an additional dose of nicotine (1 mg/kg) was injected to investigate the potential synergistic effects of combining cannabis extract with nicotine. The average of the N40 response in sham-exposed animals showed the second click to be consistently smaller in amplitude compared to the first click ($F(1,10)=29.9$, $p=2.7e{-}04$; Supplemental Figure S2A, left). This significant attenuation on the second click was also observed for noise-exposed ($F(1,10)=11.2$, $p=7e{-}03$; Supplemental Figure S2A, right). The second click attenuation differed in strength depending on the pharmacological treatment between sham and noise-exposed mice ($F(3,60)=3.67$, $p=1.7e{-}02$; Supplemental Figure S2A). For noise-exposed animals, the second click

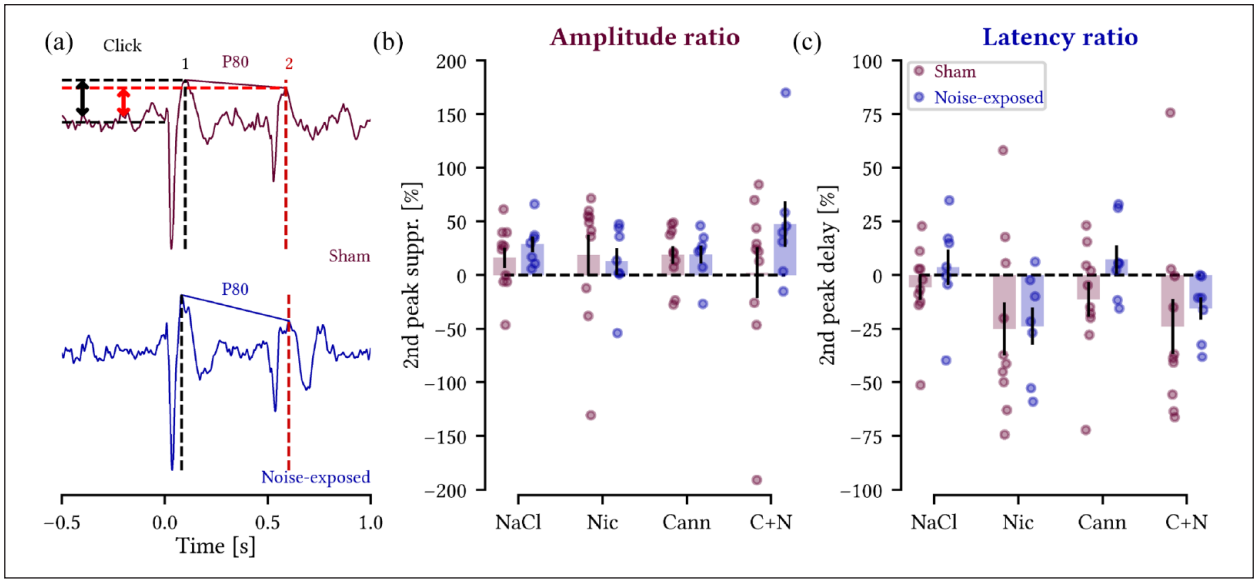

Figure 5. The P80 aERP amplitude and latency were not affected by noise-exposure or by nicotine and/or cannabis extract treatment. (a) Representative trace highlighting the P80 component (vertical black and red dashed lines for first and second clicks, respectively). Arrows represent the calculated amplitude for each P80 response for the top trace. (b) The percentage of second peak amplitude suppression showed no difference between sham and noise-exposed mice. (c) Second P80 peak delay (ratio of the 1st and 2nd click responses latencies) for sham (purple) and noise-exposed (blue) animals showed no difference between groups or treatments. A negative "delay" refers to a peak advancement. Wilcoxon signed-rank test, $n=10$ sham and seven noise-exposed mice, $p>0.05$ for all comparisons.

response was decreased compared to the first in nicotine ($p=1.6e{-}02$) and cannabis extract + nicotine ($p=1.6e{-}02$) treatment but not in saline ($p=0.237$) or cannabis extract alone ($p=0.216$; Supplemental Figure S2A, right), in contrast to sham animals. We thereby found a significant interaction between treatment and animal condition (sham or noise-exposed) on the N40 suppression ratio ($F(3,60)=3.5$, $p=2e{-}02$, Figure 4(b)). Looking specifically at sham mice, no significant difference was found in the N40 aERP ratio between treatments, while for noise-exposed animals, pairwise comparisons showed an increased N40 amplitude ratio after administration of cannabis extract + nicotine compared to cannabis extract alone ($p=1.9e{-}02$), nicotine alone ($p=3.2e{-}02$), and NaCl treatment ($p=1.9e{-}02$, Figure 4(b)). There was also a significant difference in N40 ratio under cannabis extract + nicotine treatment between sham and noise-exposed mice ($p=1.0e{-}02$; Figure 4(b)). We found a general effect of group in the N40 amplitude, where noise-exposed animals consistently showed a greater average when compared to sham-exposed mice ($F(1,20)=7.467$; $p=6.3e{-}03$; Figure 4(c), Supplemental Table S1). Taken together, these results indicate that nicotine has a more pronounced effect on the filtering of repetitive stimuli in noise-exposed animals compared to sham animals, and that the combination of nicotine + cannabis extract strongly enhances the first and second click ratio in noise-exposed animals, an effect not seen in sham animals.

Examining latency of the N40 component showed no differences in pairwise comparisons between clicks after any particular treatment ($p>0.05$; Supplemental Figure S2B), although the distribution of latencies showed the second N40 latency to be consistently shorter compared to the first ($p=2.6e{-}03$, Friedman test). Comparing the ratio of the first and second click latency revealed an increased response-delay in noise-exposed animals under cannabis treatment compared to sham animals in the same treatment ($p=3.0e{-}03$) and compared to noise-exposed mice after nicotine administration ($p=3.2e{-}02$; Figure 4(d)). This shows that cannabis delays the N40 latency compared to nicotine in noise-exposed animals but not in sham animals (Figure 4(d)). Overall, an effect of group on latency was found, where latency was consistently increased for noise-exposed mice ($p=4.3e{-}02$, Kruskal–Wallis test; Figure 4(e), Supplemental Table S2).

The P80 component of auditory aERP has been implicated in the N-methyl-D-aspartate (NMDA) dysfunction theory in schizophrenia, as ketamine can alter the P80 amplitude of mice (Connolly et al., 2004). The P80 component in response to the second click was consistently smaller compared to the response to the first stimulus ($F(1,20)=6.156$, $p=2.2e{-}02$). Also, the latency for the peak was reduced by the repetition of stimuli for both groups and all treatments ($F(1,20)=9.79$, $p=5.2e{-}03$). However, pairwise comparisons did not show any statistical differences for the P80 baseline to peak amplitude or latency (Figure 5(a); Supplemental Figure S3) nor in ratios between the two clicks for the P80 amplitude (Figure 5(b)) and latency (Figure 5(c)). This indicates that the P80 component is not affected by noise-induced tinnitus.

As previous studies suggested that the improvement of sensory gating by pharmacological agents is mediated by an enhancement of the first click rather than by the suppression of the second click (Amann et al., 2008; Rudnick et al., 2010), we separated the analysis of aERPs to focus on each click response (first; click 1 and repeated; click 2) by comparing the amplitude and latency of the N40 or P80 components between different treatments (Figure 6; Supplemental Figure S4). First, we found that sham animals increased the response to the first click after cannabis extract + nicotine treatment compared to just nicotine administration ($p=4e{-}03$; Figure 6(a), top left). Next, examining the repeated click 2 response, showed that the cannabis extract

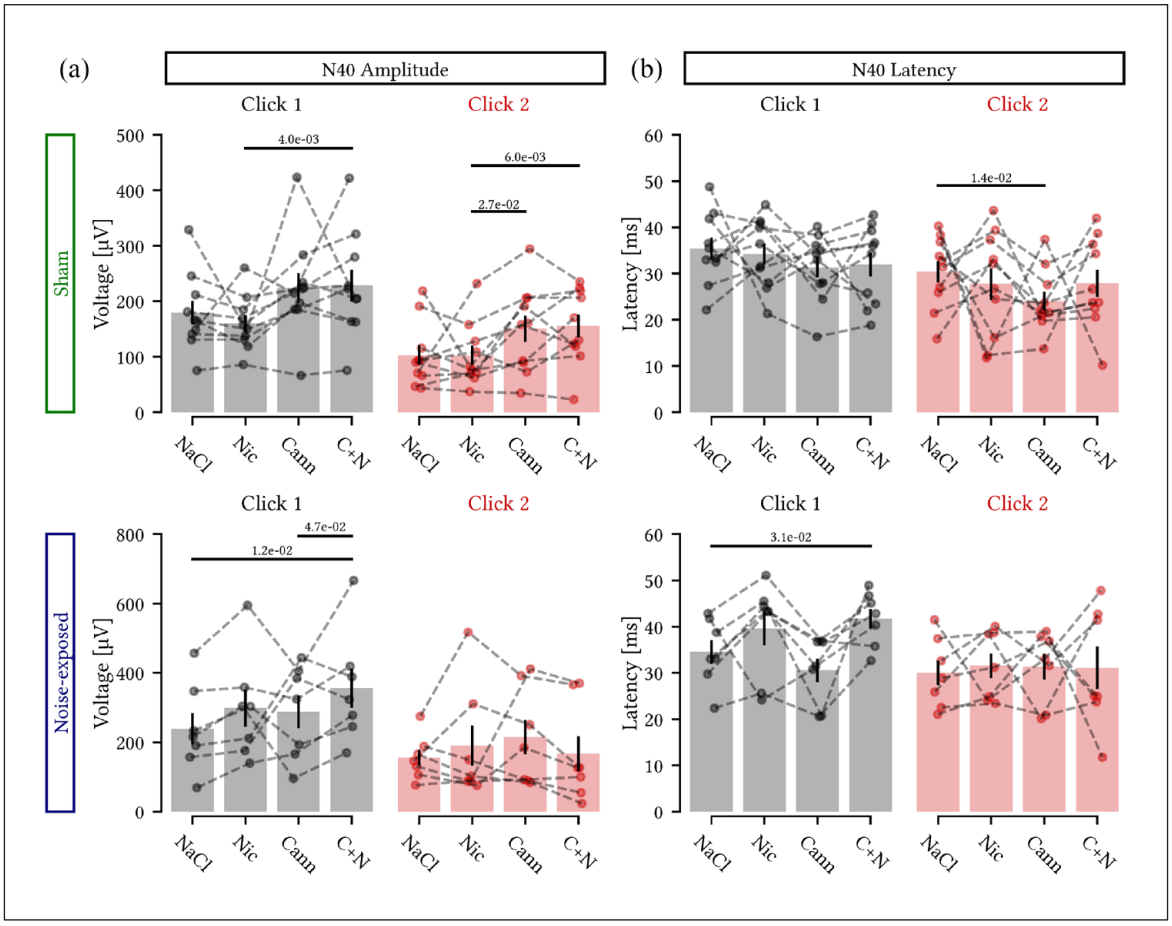

Figure 6. Noise-exposed mice only show modulation of the first click N40 response following cannabis + nicotine treatment. (a) Comparison of the N40 amplitude in response to the first click (left) and second click (right) after saline, nicotine, cannabis extract, and cannabis + nicotine administration for sham (top) and noise-exposed (bottom) mice. (b) Latency comparisons between the first (left) and second (right) click responses in sham (top) and noise-exposed (bottom) animals across treatments. Only sham animals showed alterations in the second click amplitude and latency upon nicotine and cannabis treatment. Student's *t*-test (a) and Wilcoxon signed-rank test (b), $n=10$ sham and seven noise-exposed mice.

increased the N40 click 2 response amplitude compared to nicotine ($p=2.7e{-}02$) and cannabis extract + nicotine also increased the N40 click 2 amplitude compared to nicotine alone ($p=6e{-}03$; Figure 6(a), top right). For the noise-exposed group, the combination of cannabis extract + nicotine increased click 1 amplitude compared to NaCl ($p=1.2e{-}02$; Figure 6(a), bottom left). There was no increase in click 1 response by nicotine, but still nicotine had an effect in the combination of cannabis extract since the combination of the two increased the response amplitude significantly compared to cannabis extract alone ($p=4.7e{-}02$; Figure 6(a), bottom left). The second click was unaltered by nicotine and/or cannabis extract for noise-exposed mice (Figure 6(a), bottom right). Examining the latency of the N40 response to the first click showed no alteration by either treatment in the sham group (Figure 6(b), top left). For the repeated click 2 latency, the sham group instead showed decreased latency in the presence of cannabis extract compared to NaCl treatment ($p=1.4e{-}02$; Figure 6(b), top right). For the noise-exposed group, cannabis extract + nicotine significantly delayed the click 1 N40 response compared to NaCl ($p=3.1e{-}02$; Figure 6(b), bottom left). Again, the latency of the second click N40 response was not affected by nicotine and/or cannabis extract in noise-exposed mice (Figure 6(b), bottom right). Next, examining the P80 amplitude and latency in detail only showed one effect on the second click latency for noise-exposed mice where cannabis extract + nicotine marginally increased the latency of P80 click 2 response compared to nicotine alone ($p=4.9e{-}02$; Supplemental Figure S4). All together we found the repeated second click N40 response to not be consistently modulated by treatment in noise-exposed mice, thereby agreeing with previous literature that pharmacological improvement of sensory gating affects the first click response for this set of animals (Amann et al., 2008; Rudnick et al., 2010).

Lastly, we quantified the inter-peak interval (latency between the N40 and P80 peaks) of the response to the paired clicks (Supplemental Figure S5). When double peaks were present, we measured latency from the first peak in the doublet (Supplemental Figure S5A). We did not see any difference in the number of double N40 peaks recorded from sham and noise-exposed animals ($p>0.07$ for all conditions tested; Supplemental Figure S5B). Also, there were no significant differences in the inter-peak interval between negative and positive aERP for either treatments or groups ($F(1,20)<2.06$, $p>0.1$; Supplemental Figure S5C).

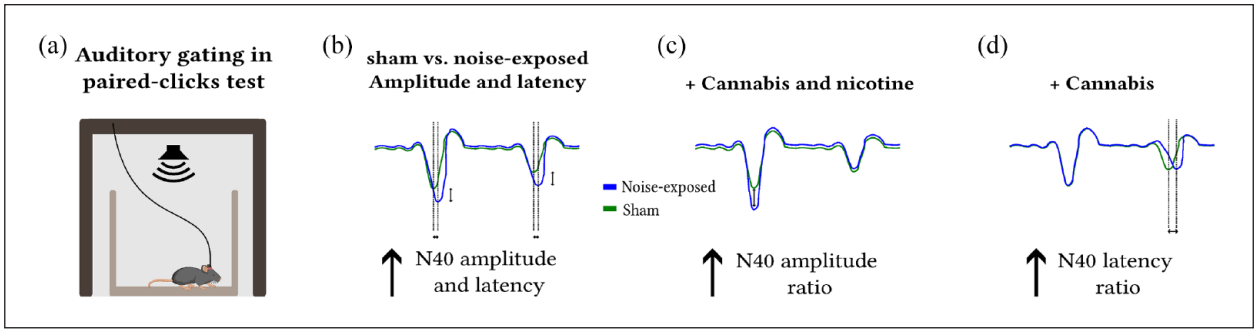

Figure 7. Schematics of the main findings. (a) Experimental setup showing an implanted animal during the paired-click test recording. (b) N40 amplitude and latency are increased in noise-exposed animals compared to sham. (c) Cannabis + nicotine treatment improved N40 ratio by increasing the first click response. (d) Cannabis treatment increased the second click latency ratio for noise-exposed animals compared to sham.

Thereby the average aERP waveform appears robust for latencies, despite individual variability.

Taken together, this study found noise-exposed mice to normally gate repetitive auditory stimuli, but showing larger amplitudes and slower processing of attention to repetitive clicks after pharmacological perturbations of the cholinergic and endocannabinoid systems, compared to sham-treated animals. The modulation of aERPs under cannabis + nicotine treatment was specifically related to the first click of the N40 component amplitude in noise-exposed mice.

Discussion

We found that the N40 amplitude and latency are increased in animals with mild noise-exposure (Figure 7(a) and (b)). These mice showed increased ratio of the amplitude of first and second click N40 components upon cannabis and nicotine administration compared to sham animals (Figure 7(c)), which indicates improvement in sensory gating. Cannabis administration also increased the latency ratio of the N40 component of aERPs for noise-exposed mice compared to sham mice (Figure 7(d)), indicating altered temporal processing. Our findings imply that cholinergic and endocannabinoid signaling and/or downstream pathways are involved in perturbed sound processing after mild noise exposure. Still, the cannabis extract may contain substances that act on non-endocannabinoid targets (Filipiuc et al., 2021), and further studies utilizing isolated endocannabinoid receptor agonists could elucidate the involvement of these receptors in sound processing.

Tinnitus is a highly heterogeneous disorder in humans (Cederroth et al., 2019), and the underlying pathophysiological mechanisms remain unclear. Recent evidence in animals and humans cumulate toward the involvement of the limbic system in tinnitus (Chen et al., 2015); however, the confounding effects of hearing loss and hyperacusis make the disentangling of each contributing factor quite challenging (Khan et al., 2021). Our data is consistent with findings described by Campbell et al. (2018), studying young individuals with mild tinnitus and a normal audiogram. They found poorer auditory processing, indicating impaired sensory gating, due to no significant difference between response amplitudes of the first and second P50 aERP for tinnitus patients (Campbell et al., 2018), similar to what we found for N40 under saline treatment (Supplemental Figure S2). Thereby our animal model results match patients with mild tinnitus. To our knowledge, this is the first study to investigate sensory gating in the hippocampus in noise-exposed mice and to evaluate how the cholinergic and endocannabinoid system interferes with sensory gating in these animals. A strength of this study is that hippocampal location for quantifying aERPs was standardized by anatomical post hoc examination and by electrophysiological profile (Scheffer-Teixeira et al., 2011) at each treatment session, thereby opening up for systematically testing a variety of compounds affecting limbic processing of attention to sound.

Another limitation is that the direct impact of nicotine and the cannabis extract on tinnitus was not assessed after the pharmacological intervention. This limitation was due to the size of the implanted electrode, thereby not allowing animals to enter the restraining tube, designed to make mice stand on all four paws during GPIAS measurements. Previous studies of cannabis as a tinnitus treatment have shown conflicting results (Narwani et al., 2020; Zheng and Smith, 2019). For instance, acute injection of the synthetic CB1/CB2 receptor agonists (WIN55,212-2, or CP55,940), exacerbates salicylate-induced tinnitus in rats assessed using a conditioned lick suppression paradigm (Zheng et al., 2010), whereas acute treatment with the CB1 receptor agonist arachidonyl-2-chloroethylamide (ACEA) had no effect (as measured by GPIAS) in guinea pigs with salicylate-induced tinnitus (Berger et al., 2017). It is possible that the confounding effects of stress on GPIAS measures caused by either salicylate or cannabis complexify the behavioral interpretation.

Based on the hypothesis that tinnitus can be similar to epilepsy due to hyperactivity in auditory and non-auditory pathways (Smith and Zheng, 2016), here we used an extract containing a high dose of THC, since it was previously demonstrated that high THC doses presented anticonvulsant effects. 50 mg/kg THC was shown to prevent spontaneous seizures in rodents (Ham et al. 1975; Rosenberg et al., 2017); and THC doses up to 100 mg/kg, with effective dose at 48 mg/kg, to be anticonvulsant after seizure generation by electroshock in mice (Wallace et al., 2001). Even 80 mg/kg THC effectively suppressed pharmacologically induced convulsions, delayed their onset, and prevented mortality in mice (Sofia et al., 1976). In addition, 96% of patients in a Canadian study reported that they would consider cannabis as a treatment for their tinnitus (Mavedatnia et al., 2023). Furthermore, cannabis extract concentration has shown *U*-shaped dose-response antidepressant effects in mice (El-Alfy et al., 2010), thereby

evaluating dose-dependent effects of activating CB1 receptors in different tinnitus models, as well as comparisons of administration routes of cannabis extract, is necessary in future studies.

Here we found that pharmacological manipulations of aERPs with both nicotine and cannabis extract improve sensory gating in noise-exposed mice but not in sham-treated animals. Our findings suggest that the higher N40 ratio under cannabis extract together with nicotine treatment in noise-exposed mice is related to an elevated click 1 amplitude and a lack of consistent modulation of the response to the second click, suggesting an increased registration (sensorial input processing) of the stimulus, as suggested previously (Brockhaus-Dumke et al., 2008). Probably this effect was not seen in sham animals because both clicks were modulated by the treatments containing cannabis.

Nicotine is known to increase the amplitude of the P20 and N40 first click in mice (Featherstone et al. 2012; Rudnick et al., 2010). The second click response has instead been shown to be sensitive to muscarinic receptor antagonists, increasing the second click amplitude, and disrupting sensory gating (Klinkenberg et al., 2011). Next, the P80 response is known to be reduced by NMDA receptor antagonists such as ketamine (Connolly et al., 2004; Featherstone et al., 2015). Thereby, an active cholinergic system appears to facilitate auditory gating of the N40 response, but it is important to notice that smoking is associated with greater risk of tinnitus (Biswas et al., 2022). We speculate that for tinnitus models nicotine might suppress hyperactivity in the dorsal cochlear nucleus since it has been previously demonstrated that cholinergic agonists such as carbachol can suppress noise-induced hyperactivity in the DCN in rodents (Manzoor et al., 2013), possibly affecting sound processing in higher areas.

The combination of cannabis extract and nicotine could potentially cause interaction effects, since it has been shown in isolated cells that anandamide (an endogenous CB1 receptor agonist) decreased nicotinic currents generated by nicotinic $\alpha 7$ and $\alpha 4\beta 2$ subunit containing acetylcholine receptors (Spivak et al., 2007). Also, a link between cannabis dependency and activity of subtypes of nicotinic acetylcholine receptors has recently been shown (Demontis et al. 2019; Donvito et al., 2018). Furthermore, the interplay between the cholinergic and endocannabinoid system has been shown in basal forebrain cholinergic neurons expressing CB1 receptors (Harkany et al., 2003) and interestingly, human subjects administered orally a combination of a THC analog and nicotine have shown improved auditory deviant detection and mismatch negativity aERPs, but not when each drug was delivered alone (de la Salle et al., 2019). Since we found only noise-exposed animals to improve N40 amplitude gating ratio in response to cannabis + nicotine treatment, and since it has been demonstrated that vesicular acetylcholine transporters puncta density is decreased on both sides of the hippocampus after noise exposure (Zhang et al., 2018b), we hypothesize that nicotine administration could be compensating for a decrease in acetylcholine release in these animals. Still, the cellular mechanisms underlying such alterations in sensory gating remain to be further investigated.

In general, the endocannabinoid system dampens neuronal activity by activation of Gi-protein coupled presynaptic CB1 receptors that decrease neurotransmitter release through blocking of presynaptic voltage-gated calcium channels and opening of voltage-gated potassium (GIRK) channels, allowing potassium to flow out of the terminal (Kendall and Yudowski, 2017). For example, high doses of natural cannabis extracts can reduce neuronal hyperactivity in in vitro models of spasticity and epilepsy (Wilkinson et al., 2003), which is interesting since noise-induced tinnitus is related to neuronal hyperactivity of the auditory system (Shore et al., 2016). Still, the circuit effect of CB1 receptor activation depends on what type of presynaptic neuron expresses CB1 receptors (e.g., glutamatergic or GABAergic cells), which can affect local plasticity differently (KANO, 2014). It is known that pyramidal cells of the hippocampus have relatively low expression of CB1 receptors (Kano et al., 2009); therefore, we expect the cannabis extract to increase auditory input due to decreased inhibition, since CB1 receptors are strongly coexpressed with GAD65 in the hippocampus (Kano et al., 2009; Li et al., 2020), especially with strong CB1 receptor expression on cholecystokinin-positive interneurons (Li et al., 2020). Furthermore, this study uses a THC-rich extract, which needs to be put in contrast to anxiolytic evaluation of THC at much lower doses (Kasten et al., 2019) and studies of seizure reduction by THC at doses as high as 100 mg/kg (Rosenberg et al., 2017). Still, the concentration of THC in a cannabis extract cannot be compared to THC alone, but should be considered in relation to other cannabinoids present. For example, a systematic review of cannabinoid treatment of chronic pain found products with high-THC-to-CBD ratios the most useful for short-term relief of neuropathic chronic pain (McDonagh et al., 2022).

The ability to suppress repetitive auditory stimuli was preserved in noise-exposed mice, suggesting that noise-induced tinnitus without changes in hearing thresholds does not interfere with auditory gating but that noise-induced tinnitus renders the response to auditory clicks abnormal in the presence of cannabis by delaying temporal coding. Here we found that cannabis alone did not decrease aERP amplitude as has been seen in human P300, probably due to the N40 component (human N100) reflecting triggered attention (Näätänen, 1992) and the human P300 reflecting cognitive stimulus classification (Bäcker et al., 2010). It is important to pin-point cellular contribution to the aERP components and here, due to the availability of a transgenic line targeting Cre expression at cells expressing the alpha-2 nicotinic receptor Leão et al., 2012), the role of the cholinergic system in sensory gating and tinnitus could be investigated by using chemogenetics to locally manipulate the excitability of these cells during aERP recordings; or in tinnitus induction performing similar manipulations during noise exposure. A similar approach would be difficult for investigating the role of the endocannabinoid system in tinnitus due to the unavailability of specific targeting of, for example, CB1-expressing cells. However, the depletion of glutamate aspartate transporter (GLAST) to exacerbate the tinnitus phenotype, may also be more appropriate to investigate in greater detail the underlying cellular and molecular mechanisms (Yu et al., 2016). Still, it is becoming clear that loud noise activates both auditory and limbic pathways (Zhang et al., 2018a) but how prolonged noise-exposure alters sound processing of each system needs to be further examined, as well as how the limbic and auditory systems interact in tinnitus (Qu et al., 2019).

In conclusion, our study shows that provoking aERP pharmacologically, using nicotine and/or cannabis extract rich in THC, showed noise-exposed mice to improve gating of the N40 component, especially under the combined influence of cannabis extract and nicotine, by increasing the first click response amplitude. However, cannabis extract also increased the latency ratio of the N40 component in

noise-exposed mice compared to sham animals, indicating delayed temporal processing of paired clicks. Thereby the activation of the cholinergic and endocannabinoid receptors and downstream pathways have distinct and different effects on auditory gating in the context of tinnitus phenotype. Our findings provide insights into the neural processing alterations associated with tinnitus-like behavior, which may facilitate the future development of diagnostic methods and potential pharmacological interventions.

Declaration of conflicting interests

The author(s) declared no potential conflicts of interest with respect to the research, authorship, and/or publication of this article.

Funding

The author(s) disclosed receipt of the following financial support for the research, authorship, and/or publication of this article: This work is supported by the American Tinnitus Association and the Brazilian funding agency CAPES - Coordenação de Aperfeiçoamento de Pessoal de Nível Superior. CRC is supported by the GENDER-Net Co-Plus Fund (GNP-182), the European Union's Horizon 2020 Research and Innovation Programme, Grant Agreement No 848261 and the European Union's Horizon 2020 research and innovation programme under the Marie Skłodowska-Curie grant agreement No 722046. TM is supported by the Wenner-Gren Stiftelserna (UPD2020-0006 and UPD2021-0114).

ORCID iDs

Barbara Ciralli https://orcid.org/0000-0003-4021-2668
Thawann Malfatti https://orcid.org/0000-0001-9672-9995
Thiago Z. Lima https://orcid.org/0000-0003-2039-0205
Sérgio Ruschi B. Silva https://orcid.org/0000-0003-0677-0439
Katarina E. Leao https://orcid.org/0000-0001-7295-1233

Data availability statement

The datasets generated and/or analyzed in the current study are available on request.

Supplemental material

Supplemental material for this article is available online.

References

Amann LC, Phillips JM, Halene TB, et al. (2008) Male and female mice differ for baseline and nicotine-induced event related potentials. *Behav Neurosci* 122: 982–990.

Asokan MM, Williamson RS, Hancock KE, et al. (2018) Sensory overamplification in layer 5 auditory corticofugal projection neurons following cochlear nerve synaptic damage. *Nat Commun* 9: 2468.

Bäcker K, Gerritsen J, Hunault C, et al. (2010) Cannabis with high δ9-thc contents affects perception and visual selective attention acutely: An event-related potential study. *Pharmacol Biochem Behav* 96: 67–74.

Ballinger EC, Ananth M, Talmage DA, et al. (2016) Basal forebrain cholinergic circuits and signaling in cognition and cognitive decline. *Neuron* 91: 1199–1218.

Berger JI, Coomber B, Hill S, et al. (2017) Effects of the cannabinoid cb 1 agonist ACEA on salicylate ototoxicity, hyperacusis and tinnitus in guinea pigs. *Hear Res* 356: 51–62.

Biswas R, Lugo A, Akeroyd MA, et al. (2022) Tinnitus prevalence in Europe: A multi-country cross-sectional population study. *Lancet Reg Health-Eur* 12: 100250.

Brockhaus-Dumke A, Schultze-Lutter F, Mueller R, et al. (2008) Sensory gating in schizophrenia: P50 and n100 gating in antipsychotic-free subjects at risk, first-episode, and chronic patients. *Biol Psychiatry* 64: 376–384.

Campbell J, Bean C and LaBrec A (2018) Normal hearing young adults with mild tinnitus: Reduced inhibition as measured through sensory gating. *Audiol Res* 8: 214.

Cederroth CR, PirouziFard M, Trpchevska N, et al. (2019) Association of genetic vs environmental factors in Swedish adoptees with clinically significant tinnitus. *JAMA Otolaryngol Head Neck Surg* 145: 222.

Cenquizca LA and Swanson LW (2007) Spatial organization of direct hippocampal field ca1 axonal projections to the rest of the cerebral cortex. *Brain Res Rev* 56: 1–26.

Chen YC, Li X, Liu L, et al. (2015) Tinnitus and hyperacusis involve hyperactivity and enhanced connectivity in auditory-limbic-arousal-cerebellar network. *Elife* 4: e06576.

Cima RFF, Mazurek B, Haider H, et al. (2019) A multidisciplinary European guideline for tinnitus: Diagnostics, assessment, and treatment. *HNO* 67: 10–42.

Ciralli B, Malfatti T and Lima TZ (2022) *Sensory Gating On Tinnitus 2022*. Git repository. https://gitlab.com/bciralli/sensorygatingontinnitus2022

Connolly PM, Maxwell C, Liang Y, et al. (2004) The effects of ketamine vary among inbred mouse strains and mimic schizophrenia for the p80, but not p20 or n40 auditory erp components. *Neurochem Res* 29: 1179–1188.

de la Salle S, Inyang L, Impey D, et al. (2019) Acute separate and combined effects of cannabinoid and nicotinic receptor agonists on MMN-indexed auditory deviance detection in healthy humans. *Pharmacol Biochem Behav* 184: 172739.

Demontis D, Rajagopal VM, Thorgeirsson TE, et al. (2019) Genome-wide association study implicates chrna2 in cannabis use disorder. *Nat Neurosci* 22: 1066–1074.

Dissanayake DW, Zachariou M, Marsden CA, et al. (2008) Auditory gating in rat hippocampus and medial prefrontal cortex: Effect of the cannabinoid agonist win55,212-2. *Neuropharmacology* 55: 1397–1404.

Donvito G, Muldoon PP, Jackson KJ, et al. (2018) Neuronal nicotinic acetylcholine receptors mediate δ9-thc dependence: Mouse and human studies. *Addict Biol* 25: e12691.

dos Santos Filha VAV and Matas CG (2010) Late auditory evoked potentials in individuals with tinnitus. *Brazil J Otorhinolaryngol* 76: 263–270.

El-Alfy AT, Ivey K, Robinson K, et al. (2010) Antidepressant-like effect of δ9-tetrahydrocannabinol and other cannabinoids isolated from cannabis sativa l. *Pharmacol Biochem Behav* 95: 434–442.

Featherstone RE, Phillips JM, Thieu T, et al. (2012) Nicotine receptor subtype-specific effects on auditory evoked oscillations and potentials. *PLoS One* 7: e39775.

Featherstone RE, Shin R, Kogan JH, et al. (2015) Mice with subtle reduction of NMDA NR1 receptor subunit expression have a selective decrease in mismatch negativity: Implications for schizophrenia prodromal population. *Neurobiol Dis* 73: 289–295.

Filipiuc LE, Ababei DC, Alexa-Stratulat T, et al. (2021) Major phytocannabinoids and their related compounds: Should we only search for drugs that act on cannabinoid receptors? *Pharmaceutics* 13: 1823.

Ham MT, Loskota WJ and Lomax P (1975) Acute and chronic effects of δ9-tetrahydrocannabinol on seizures in the gerbil. *Eur J Pharmacol* 31: 148–152.

Harkany T, Hartig W, Berghuis P, et al. (2003) Complementary distribution of type 1 cannabinoid receptors and vesicular glutamate transporter 3 in basal forebrain suggests input-specific retrograde signalling by cholinergic neurons. *Eur J Neurosci* 18: 1979–1992.

Harris CR, Millman KJ, van der Walt SJ, et al. (2020) Array programming with NumPy. *Nature* 585: 357–362.

Henry KR (1979) Auditory brainstem volume-conducted responses: Origins in the laboratory mouse. *J Am Aud Soc* 4: 173–178.

Hiller W and Goebel G (2006) Factors influencing tinnitus loudness and annoyance. *Arch Otolaryngo Head Neck Surg* 132: 1323.

Hunter JD (2007) Matplotlib: A 2d Graphics Environment. *Comput Sci Eng* 9: 90–95.

Inkscape Project (2022) Inkscape. *URL* https://inkscape.org.Software.

Johansson E, Ohlsson A, Lindgren JE, et al. (1987) Single-dose kinetics of deuterium-labelled cannabinol in man after intravenous administration and smoking. *Biol Mass Spectr* 14: 495–499.

KANO M (2014) Control of synaptic function by endocannabinoid-mediated retrograde signaling. *Proc Jpn Acad Ser B* 90: 235–250.

Kano M, Ohno-Shosaku T, Hashimotodani Y, et al. (2009) Endocannabinoid-mediated control of synaptic transmission. *Physiol Rev* 89: 309–380.

Kasten CR, Zhang Y and Boehm SL (2019) Acute cannabinoids produce robust anxiety-like and locomotor effects in mice, but long-term consequences are age- and sex-dependent. *Front Behav Neurosci* 13: 32.

Kendall DA and Yudowski GA (2017) Cannabinoid receptors in the central nervous system: Their signaling and roles in disease. *Front Cell Neurosci* 10: 294.

Khan RA, Sutton BP, Tai Y, et al. (2021) A large-scale diffusion imaging study of tinnitus and hearing loss. *Sci Rep* 11: 23395.

Klinkenberg I, Sambeth A and Blokland A (2011) Acetylcholine and attention. *Behav Brain Res* 221: 430–442.

Langguth B, Landgrebe M, Kleinjung T, et al. (2011) Tinnitus and depression. *World J Biol Psychiatry* 12: 489–500.

Lanting C, de Kleine E and van Dijk P (2009) Neural activity underlying tinnitus generation: Results from pet and FMRI. *Hear Res* 255: 1–13.

Leão RN, Mikulovic S, Leão KE, et al. (2012) OLM interneurons differentially modulate CA3 and entorhinal inputs to hippocampal CA1 neurons. *Nat Neurosci* 15: 1524–1530.

Li H, Yang J, Tian C, et al. (2020) Organized cannabinoid receptor distribution in neurons revealed by super-resolution fluorescence imaging. *Nat Commun* 11: 5699.

Li S, Choi V and Tzounopoulos T (2013) Pathogenic plasticity of kv7.2/3 channel activity is essential for the induction of tinnitus. *Proc Natl Acad Sci* 110: 9980–9985.

Lijffijt M, Lane SD, Meier SL, et al. (2009) P50, n100, and p200 sensory gating: Relationships with behavioral inhibition, attention, and working memory. *Psychophysiology* 46: 1059–1068.

Longenecker R and Galazyuk A (2012) Methodological optimization of tinnitus assessment using prepulse inhibition of the acoustic startle reflex. *Brain Res* 1485: 54–62.

Longenecker RJ and Galazyuk AV (2016) Variable effects of acoustic trauma on behavioral and neural correlates of tinnitus in individual animals. *Front Behav Neurosci* 10: 207.

Longenecker RJ, Kristaponyte I, Nelson GL, et al. (2018) Addressing variability in the acoustic startle reflex for accurate gap detection assessment. *Hear Res* 363: 119–135.

Ma J, Tai SK and Leung LS (2009) Ketamine-induced deficit of auditory gating in the hippocampus of rats is alleviated by medial septal inactivation and antipsychotic drugs. *Psychopharmacology* 206: 457–467.

Malfatti T (2023) Sciscripts. Python package. https://zenodo.org/record/4045872

Malfatti T, Ciralli B, Hilscher MM, et al. (2022) Decreasing dorsal cochlear nucleus activity ameliorates noise-induced tinnitus perception in mice. *BMC Biol* 20: 102.

Manzoor N, Gao Y, Licari F, et al. (2013) Comparison and contrast of noise-induced hyperactivity in the dorsal cochlear nucleus and inferior colliculus. *Hear Res* 295: 114–123.

Mavedatnia D, Levin M, Lee JW, et al. (2023) Cannabis use amongst tinnitus patients: Consumption patterns and attitudes. *J Otolaryngol Head Neck Surg* 52: 19.

McDonagh MS, Morasco BJ, Wagner J, et al. (2022) Cannabis-based products for chronic pain: A systematic review. *Ann Intern Med* 175: 1143–1153.

Metzger KL, Maxwell CR, Liang Y, et al. (2007) Effects of nicotine vary across two auditory evoked potentials in the mouse. *Biol Psychiatry* 61: 23–30.

Näätänen R (1992) *Attention and Brain Function*. London. Psychology Press.

Nadhimi Y and Llano DA (2021) Does hearing loss lead to dementia? A review of the literature. *Hear Res* 402: 108038.

Narwani V, Bourdillon A, Nalamada K, et al. (2020) Does cannabis alleviate tinnitus? A review of the current literature. *Laryngosc Invest Otolaryngol* 5: 1147–1155.

Park SY, Kim MJ, Park JM, et al. (2020) A mouse model of tinnitus using gap prepulse inhibition of the acoustic startle in an accelerated hearing loss strain. *Otol Neurotol* 41: e516–e525.

Petersen D, Norris K and Thompson J (1984) A comparative study of the disposition of nicotine and its metabolites in three inbred strains of mice. *Drug Metabol Dispos* 12: 725–731.

Qu T, Qi Y, Yu S, et al. (2019) Dynamic changes of functional neuronal activities between the auditory pathway and limbic systems contribute to noise-induced tinnitus with a normal audiogram. *Neuroscience* 408: 31–45.

Rosenberg EC, Patra PH and Whalley BJ (2017) Therapeutic effects of cannabinoids in animal models of seizures, epilepsy, epileptogenesis, and epilepsy-related neuroprotection. *Epil Behav* 70: 319–327.

Rudnick ND, Strasser AA, Phillips JM, et al. (2010) Mouse model predicts effects of smoking and varenicline on event-related potentials in humans. *Nicot Tobacco Res* 12: 589–597.

Sampson PB (2020) Phytocannabinoid pharmacology: Medicinal properties of cannabis sativa constituents aside from the "big two". *J Nat Prod* 84: 142–160.

Scheffer-Teixeira R, Belchior H, Caixeta FV, et al. (2011) Theta phase modulates multiple layer-specific oscillations in the ca1 region. *Cerebral Cortex* 22: 2404–2414.

Shore SE, Roberts LE and Langguth B (2016) Maladaptive plasticity in tinnitus—triggers, mechanisms and treatment. *Nat Rev Neurol* 12: 150–160.

Siegle JH, Hale GJ, Newman JP, et al. (2015) Neural ensemble communities: Open-source approaches to hardware for large-scale electrophysiology. *Curr Opin Neurobiol* 32: 53–59.

Smith PF and Zheng Y (2016) Cannabinoids, cannabinoid receptors and tinnitus. *Hear Res* 332: 210–216.

Smucny J, Stevens KE, Olincy A, et al. (2015) Translational utility of rodent hippocampal auditory gating in schizophrenia research: A review and evaluation. *Transl Psychiatr* 5: e587–e587.

Sofia R, Solomon TA and Barry H (1976) Anticonvulsant activity of δ9-tetrahydrocannabinol compared with three other drugs. *Eur J Pharmacol* 35: 7–16.

Spivak CE, Lupica CR and Oz M (2007) The endocannabinoid anandamide inhibits the function of α4β2 nicotinic acetylcholine receptors. *Mol Pharmacol* 72: 1024–1032.

Sturm JJ, Zhang-Hooks YX, Roos H, et al. (2017) Noise trauma-induced behavioral gap detection deficits correlate with reorganization of excitatory and inhibitory local circuits in the inferior colliculus and are prevented by acoustic enrichment. *J Neurosci* 37: 6314–6330.

Tai Y and Husain FT (2019) The role of cognitive control in tinnitus and its relation to speech-in-noise performance. *J Audiol Otol* 23: 1.

Torrens A, Vozella V, Huff H, et al. (2020) Comparative pharmacokinetics of δ9-tetrahydrocannabinol in adolescent and adult male mice. *J Pharmacol Exp Therap* 374: 151–160.

Turner J, Larsen D, Hughes L, et al. (2012) Time course of tinnitus development following noise exposure in mice. *J Neurosci Res* 90: 1480–1488.

Turner JG, Brozoski TJ, Bauer CA, et al. (2006) Gap detection deficits in rats with tinnitus: A potential novel screening tool. *Behav Neurosci* 120: 188–195.

Verrico CD, Jentsch JD, Roth RH, et al. (2003) Repeated, intermittent δ9-tetrahydrocannabinol administration to rats impairs acquisition and performance of a test of visuospatial divided attention. *Neuropsychopharmacology* 29: 522–529.

Virtanen P, Gommers R, Oliphant TE, et al. (2020) SciPy 1.0: Fundamental algorithms for scientific computing in python. *Nat Meth* 17: 261–272.

Wallace MJ, Wiley JL, Martin BR, et al. (2001) Assessment of the role of cb1 receptors in cannabinoid anticonvulsant effects. *Eur J Pharmacol* 428: 51–57.

Wilkinson JD, Whalley BJ, Baker D, et al. (2003) Medicinal cannabis: Is δ9-tetrahydrocannabinol necessary for all its effects? *J Pharm Pharm* 55: 1687–1694.

Xu C, Chang T, Du Y, et al. (2019) Pharmacokinetics of oral and intravenous cannabidiol and its antidepressant-like effects in chronic mild stress mouse model. *Environ Toxicol Pharmacol* 70: 103202.

Yu H, Patil KV, Han C, et al. (2016) GLAST deficiency in mice exacerbates gap detection deficits in a model of salicylate-induced tinnitus. *Front Behav Neurosci* 10: 158.

Zeng FG, Richardson M and Turner K (2020) Tinnitus does not interfere with auditory and speech perception. *J Neurosci* 40: 6007–6017.

Zhang GW, Sun WJ, Zingg B, et al. (2018a) A non-canonical reticular-limbic central auditory pathway via medial septum contributes to fear conditioning. *Neuron* 97: 406–417.e4.

Zhang L, Wu C, Martel DT, et al. (2018b) Remodeling of cholinergic input to the hippocampus after noise exposure and tinnitus induction in guinea pigs. *Hippocampus* 29: 669–682.

Zhang W, Peng Z, Yu S, et al. (2020) Exposure to sodium salicylate disrupts VGLUT3 expression in cochlear inner hair cells and contributes to tinnitus. *Physiol Res* 69: 181–190.

Zheng Y and Smith PF (2019) Cannabinoid drugs: Will they relieve or exacerbate tinnitus? *Curr Opin Neurol* 32: 131–136.

Zheng Y, Stiles L, Hamilton E, et al. (2010) The effects of the synthetic cannabinoid receptor agonists, win55,212-2 and cp55,940, on salicylate-induced tinnitus in rats. *Hear Res* 268: 145–150.